

A Study on the Dynamic Response of RC "L" Joint Under the Simulated Seismic Load.

模擬 地震荷重을 받는 RC "L" joint의 動的舉動에 關한 研究

朴 承 範* · 清 宮 埋**
Seung Bum Park, Osamu Kyomia

要 約

最近 鐵筋콘크리트 構造物의 地震荷重 및 이와 類似한 震動荷重에 대한 耐震安全性 問題가 대두되어 이에 關한 模型供試體의 振動實驗 및 實存構造物의 動的構造特性의 解析 等に 의한 耐震性 向上을 爲한 補強方法이 강구되고 있다.

本 研究에서는 震動荷重에 파괴되기 쉬운 鐵筋콘크리트 보와 기둥이 상호 교차되는 조인트 구역의 動的破壞舉動을 確認하기 위하여 "L"形 鐵筋콘크리트 조인트 部材를 製作, 模擬地震荷重 條件下에서의 動的 應答特性을 究明하고자 反復荷重에 따른 joint區域과 보 및 기둥의 動的破壞舉動을 考察하였다. 특히 耐震構造物 設計에 主要 要素인 延性(μ)이 0.5, 1.0, 3.0일 때 각각 3회씩 그리고 $\mu=5.0$ 일 때 部材가 完全히 파괴될 때까지 4회 반복하여 反復荷重을 作用시키면서 이때의 部材의 極限強度 및 그 變形性能을 LVDT System을 使用하여 調查分析하였으며, 破壞性狀은 勿論 配筋效果에 對하여도 이를 究明하고자 努力하였다.

本 研究 結果 무엇보다도 部材의 剛성과 耐力의 向上 및 伸縮灣曲, 剪斷變形 等の 變形性能의 改善 그리고 보의 脆破壞에 對한 補強 및 joint區域의 剪斷補強은 耐震構造物 設計를 爲하여 重要 事項임을 確認하였다.

I. Introduction

Through the years, RC design for seismic safety has continuously been advanced^{2,5,6}. A major importance in the design of a building of this sort is the intersection points where a beam or a girder may run into a column^{3,7,9,10}. This point is more formally referred to as a joint. The purpose of this experiment is to investigate the response of a RC "L" joint which is subjected to a variable vertical cyclic load applied at the tip of the beam. For seismic loads, the

ductility (μ) is an important factor in the design of RC structures. The ductility (μ) of a material or a member is often defined as the ratio of deformation at ultimate to that at yield^{4,5,12}. At this study, it will be interested to determine whether both the column and the beam are able to reach their ultimate capacities and to observe cracking and deformations under simulated seismic loading. Also this study carried out to investigate the modes of cracking, the effects of re-bar slip and working on structural response.

* 忠南大學校 工業教育大學

** 美國 캘리포니아 州立大學校

II. Description of Specimen and Equipment

1. Specimen and Equipment

The specimen is a reinforced concrete "L" joint. Joint details are shown in Fig.2. The relevant material properties of the specimen are as follows; $\sigma_y=3,585\text{kg/cm}^2$, $E_s=2,038,932\text{ kg/cm}^2$, $\sigma_c=339\text{kg/cm}^2$, $E_c=282,146\text{kg/cm}^2$.

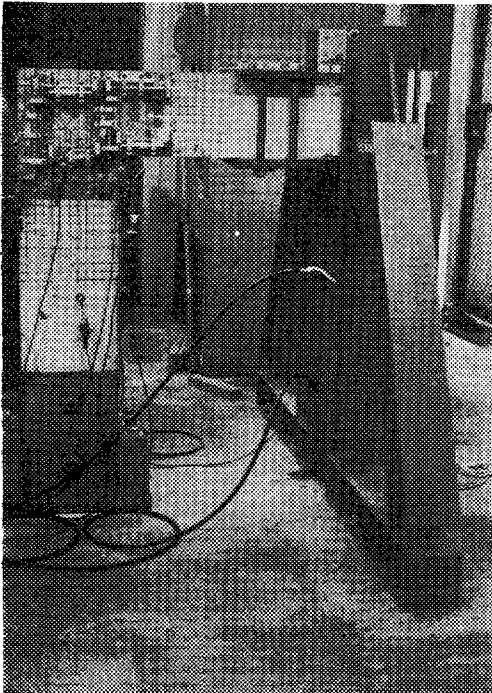


Photo. 1. Testing Equipment for Specimen

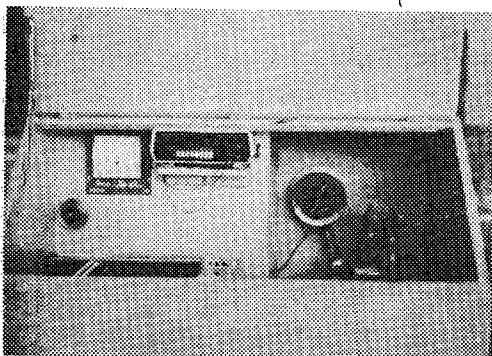


Photo. 2. Measuring Instruments for Test

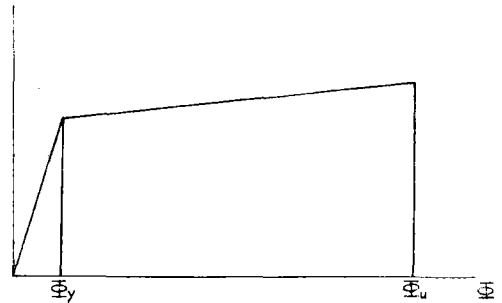


Fig. 1. Typical moment-rotation diagram (M vs. ϕ) to illustrate the definition of ductility.

Concrete Mix ratio 1 : 1.5 : 3, W/C 49%, Unit Cement 365kg/m^3 , Unit water 178kg/m^3 , G/S 1.88, Max. size of Coarse Agg. 25mm.

Instruments used in this test are 15 LVDT's, Pressure Transducer, Digital Volt Meter and X-Y recorder. LVDT's (# 1-8) are used to measure stretch and curvatures, LVDT's (# 9-14) are used to measure shear deformation and LVDT (# 15) is used to measure tip deflection. In the DVM, channels 1 through 15 are for LVDT's and channel 16 is for the reading of pressure transducer. Photo. 1,2 are the testing facilities. Fig.2 is the description of specimen and Fig.3 is the positions of LDVT's.

2. Ductility

Ductility (μ) is an important variable in the design of R.C. structures expected to experience seismic loads. Ductility of a member is defined as the ratio of deformation at ultimate to that at yield.

Ductility is important in seismic design in that a joint must sustain a moment (M_y) over a large angle of rotation so that local yielding will not over the capacity of the structure.

For this experiment, ductility will be defined as the observed tip deflection divided by the calculated tip deflection at yield. Ductility will be used as the criteria for maximum deflection at each cycle.

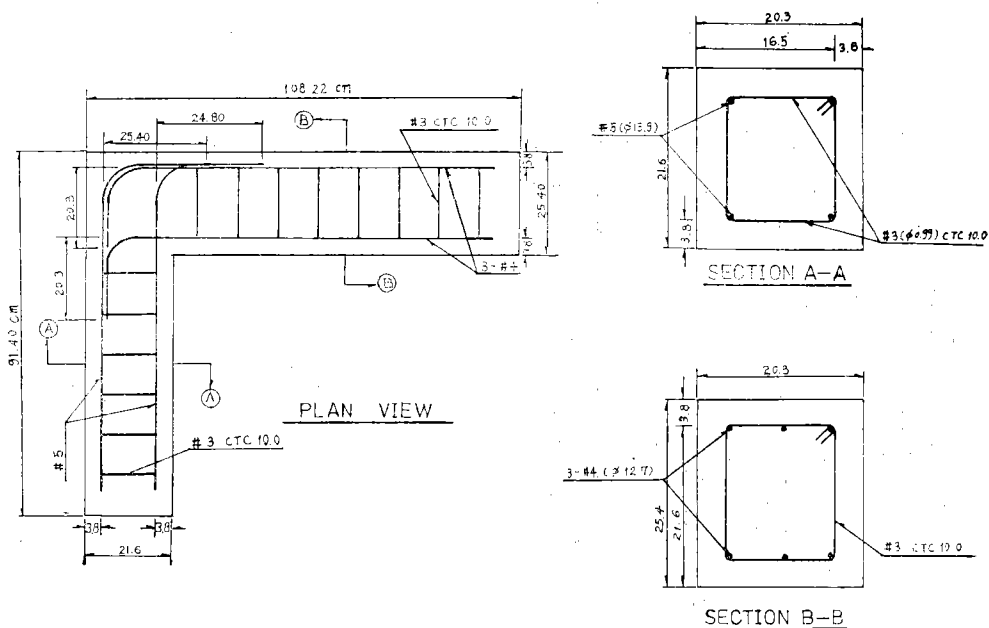


Fig. 2. Description of Specimen

III. Experimental Procedure and Pre-calculations

The objective of the procedure is to perform 3 cycles at half yield ($\mu=0.5$, $\Delta tip=0.6cm$), 3 cycles at yield loading ($\mu=1.0$, $\Delta tip=1.3cm$), 3 cycles at yield bad ($\mu=3.0$, $\Delta tip=3.9cm$) and as many at $\mu=5.0$ ($\Delta Tip=6.5cm$) until failure is complete. The ductility can be related to $\mu = \frac{\epsilon_{observed}}{\epsilon_y} (\epsilon_y = \Delta Tip)$. ΔTip (Tip displacement) can be calculated from eq. (1)¹¹⁾.

$$\Delta Tip = \int_0^l \frac{mM}{EI} dx + \int_0^l \frac{m'M}{EI} dx' \dots\dots\dots(1)$$

m = Bending Moment of column (virtual force)
 m' = Bending Moment of Beam (virtual force)

And the P_y can be related from Min. $\{P_y, B. Bend, P_y, B. Shear, P_y, Col. Bend.\}$ Min. P_y will be the value of applied load to cause initial yielding. In order to determine the yielding load for the member, all of the possible modes of failure were analyzed and the jacking force required were calculated. The values of P_y to

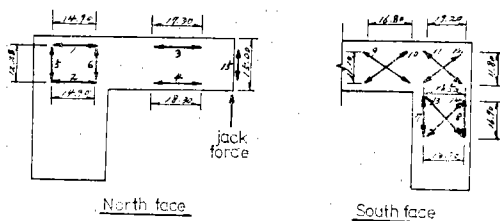


Fig. 3. Locations of LVDT's

use for the experiment is 3,400kg for yield ($\mu=1.0$, $\Delta Tip=1.3CM$) and Target pressures are 88kg/cm² for downward load and 76kg/cm² for upward load. The calculation of stretch, curvature and shear deformation are investigated on the regions for beam, joint and column. Extensions (stretch) are calculated between all parallel LVDT's (1-2, 3-4, 5-6, 7-8) by using eq. (2)

$$S = \frac{\Delta 1 + \Delta 2}{2b} \dots\dots\dots(2) \quad \frac{LVDT1}{LVDT2} \uparrow a$$

|←-b-→|

Curvatures are calculated between LVDT's (1-2, 3-4, 5-6, 7-8) by using eq. (3)

$$Cur. = \frac{\Delta 1 + \Delta 2}{ab} \dots\dots\dots(3)$$

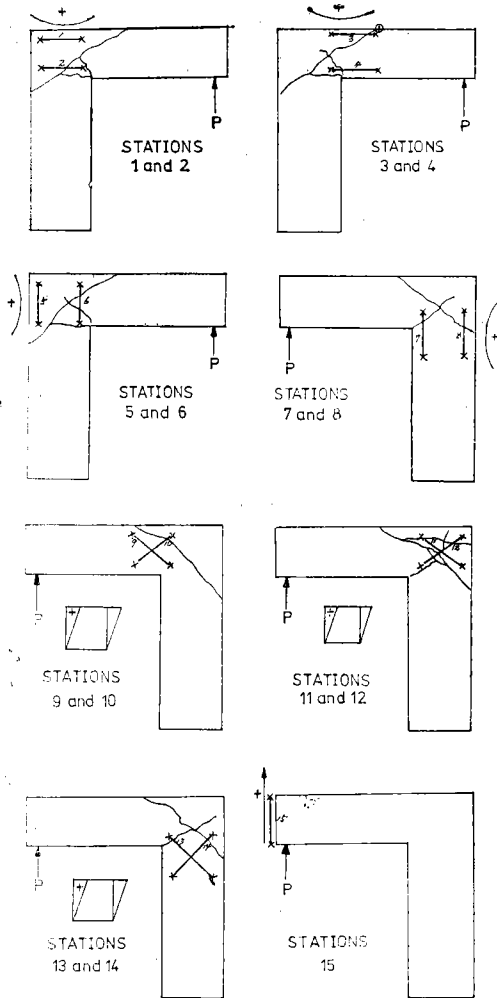
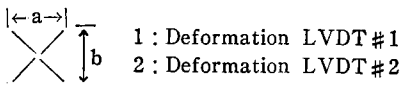


Fig. 4. Crack record at each stations

Symbol : $\Delta(+)$: Elongation
 $\Delta(-)$: Shortening

Shear deformation (r) are calculated for LVDT's (9-10, 11-12, 13-14) by using eq.(4)

$$r = \frac{(\Delta_1 - \Delta_2) \sqrt{a^2 + b^2}}{2ab} \dots\dots\dots(4)$$



IV. Interpretation of Results

1. STATION 1 and 2 (EXTENSION)

In the elastic region (Cycle 1-6; elastic beha-

avior), stations 1 and 2 extend on the down-cycle with station 1 being the dominant factor. On the up cycle, 1 and 2 tend to compress with station 1 again as the dominant factor.

In the inelastic region (Cycle 7-13; inelastic behavior), stations 1 and 2 change their stretch behavior completely with the introduction of two major shear cracks at the joint, on crack running from outside to outside of the joint puts station 1 in a unstressed isolated region of the joint, and puts the two anchoring points of station 2 on opposite sides of the crack. Another crack runs from the re-entry point towards the spex. On the down cycle, the re-entry point crack closes hence the load increases in with little change in compression. On the up cycle, the two cracks open hence the increase in extension with small change in applied load.

STATION 1 and 2(CURVATURE)

The elastic behavior is as would be expected, an almost linear relationship between curvature and applied load.

In the inelastic region, the opening and closing of the two cracks dictate the behavior as in the inelastic extension.

2. STATION 3 and 4 (EXTENSION)

The results from station 4 are meaningless for the elastic runs due to a cold solder connecting the LVDT to the console.

The linear extension curve only reflects the behavior of station 3.

In the inelastic region, it is noted that both the extension and compression are of comparable magnitude. On a close examination of the cracking pattern and the LVDT readouts, it can be seen that station 3 plays the dominant role at this location. The extension plot seeme to reflect a rigid body rotation of the beam about the joint, the pivot point being directly above the anchoring point to station 3 away from the joint.

The left anchoring point of station 4 sits in a section of the joint isolated from both the beam and the column by cracks. Basically this section

follows the beam on the up cycles and resists compression on the down cycles.

STATION 3 and 4 (CURVATURE)

In the inelastic region, the mechanism explained above is again apparent for the curvature plots. On the down cycles, the cracks close and

so the curvature is not so great, but on the up cycles, when the cracks open, the change in curvature is greatly increased.

3. STATIONS 5 and 6 (EXTENSION)

Before any cracks open, stations 5 and 6 do

Table-1. Test Results for LVDT's #1-14. (Unit : CM)

Cycle Δ	$\Delta 1$	$\Delta 2$	$\Delta 3$	$\Delta 4$	$\Delta 5$	$\Delta 6$	$\Delta 7$
DOWN	0.0170	0.1557	0.1826	0.1049	-0.0051	0.7902	0.1136
	.0330	.0267	.1755	.0470	.0033	.4691	.0455
	.0427	.0147	.1872	.0236	.0206	.4046	.0284
	.0627	.0132	.2113	.0036	.0345	.3858	.0081
	.0826	.0102	.2416	-.0018	.0411	.3825	.0005
	.1062	.0094	.2543	-.0020	.0427	.3820	-.0023
RETURN	.1082	.0094	.2885	-.0020	.0429	.3818	-.0025
	.1062	.0094	.2842	-.0020	.0432	.3810	-.0025
	.0978	.0091	.2621	-.0020	.0422	.3764	-.0023
	.0940	.0094	.2576	-.0023	.0394	.3741	-.0013
	.0813	.0097	.2497	.0137	.0292	.3693	.0081
	UP	.0805	.0097	.2497	.0137	.0293	.3693
.0503		.1318	.2433	.0983	.0155	.6619	.0953
.0521		.1864	.2357	.0988	.0130	.7925	.1096
.0579		.2377	.2309	.1156	.0117	.9340	.1250
.0612		.2758	.2286	.1359	.0150	1.0571	.1438
.0622		.3122	.2248	.1544	.0180	1.1745	.1628
.0610	.3505	.2195	.1722	.0193	1.3104	.1801	
RETURN	.0599	.3279	.2195	.1933	.0203	1.3216	.1803
	.0599	.3183	.2195	.1778	.0196	1.2962	.1801
	.0594	.2946	.2197	.1608	.0165	1.2464	.1699
	.0538	.2565	.2197	.1346	.0130	1.1641	.1547
	.0518	.1257	.2187	.1064	.0114	.9609	.1118
	DOWN	0.1638	0.0465	0.5773	0.0871	0.5705	0.0246
.0467		.0843	.4643	.1676	.2532	.0185	.1981
.0170		.1013	.4420	.1961	.2000	.0185	.1783
-.0030		.1115	.4237	.2210	.1425	.0178	.1486
-.0048		.1217	.4112	.2416	.0980	.0175	.1311
.0173		.1372	.4112	.2642	.0706	.0175	.1247
RETURN	.0218	.1461	.4044	.2657	.0678	.0175	.1222
	.0229	.1364	.4008	.2616	.0678	.0175	.1212
	.0287	.1298	.3896	.2464	.0724	.0180	.1191
	.0323	.1260	.3866	.2413	.0762	.0183	.1191
	.0625	.1021	.3503	.2164	.0909	.0226	.1214
	UP	.0648	.1021	.3503	.2144	.0914	.0226
.1615		.0884	.5222	.1173	.4404	.0315	.2352
.1915		.0859	.5941	.1143	.5453	.0284	.2728
.2144		.0833	.6843	.1186	.6513	.0282	.3162
.2314		.0813	.7402	.1222	.7435	.0282	.3561
.2525		.0790	.8054	.1214	.8270	.0282	.3881
.2764	.0770	.8440	.1186	.9243	.0282	.4267	
RETURN	.2766	.0770	.8456	.1173	.9284	.0282	.4280
	.2799	.0767	.8293	.1186	.9129	.0282	.4260
	.2581	.0770	.7973	.1181	.8750	.0269	.4069
	.2134	.0772	.7513	.1123	.8161	.0264	.3767
	.1344	.0777	.6568	.1278	.6294	.0297	.3096

not respond to any significant degree. But with the opening of shear cracks, the stations begin to respond. At cycle 4, the first ductility 1 cycle, station 6 opens on the up cycle with the appearance of the cracks and never quite recovers. After this point the behavior is similar to the 1/2 yield cycles, only displaced to the right. This can be explained by rebar slip.

In the inelastic region, the cracks again play a major role in the determination of the extension behavior. The explanation for stations 1 and 2 also hold for 5 and 6. The plastic extension strains for both 1 and 2 and 5 and 6 are of the same order of magnitude due to the dependence on the same system of cracks.

STATION 5 and 6 (CURVATURE)

The curvature diagrams hold the same general shape as the extension diagram. Hence it can be concluded that one of the two stations dominate. The dominant station being 6 which straddles the re-entry crack. Station 5 has little response since it is near a free surface and straddles no open cracks.

4. STATIONS 7 and 8 (EXTENSION)

An interesting phenomenon occurs at this station in the elastic region, the two stations never compress. Instead the two stations take turns being the pivot point for the rotation of the beam. This behavior is partially responsible for the higher load required for tip deflection on the down cycle.

At cycle 4, rebar slip and cracking and the absence of a direct compressive force prevents complete recovery.

In the inelastic region, the mechanism observed for the earlier cycles become more pronounced due to the slip of the #5 rebar running on the inside of the joint on the up cycles.

As in stations 1 and 2, and 5 and 6, the opening and closing of the diagonal shear cracks dominate the behavior of stations 7 and 8.

STATION 7 and 8 (CURVATURE)

In the elastic region, the curvature is fairly

small and recovery is almost 100%.

In the inelastic region, this station as in other stations tend to be dominated by the shear crack running from outside to outside.

5. STATIONS 9 and 10 (SHEAR DEFORMATION)

The elastic behavior is as would be expected by elastic analysis. The inelastic behavior is quite different.

As in stations 3 and 4 (which are on the other side of the member) the "rigid body rotation" mechanism seems to be in action here. On the down cycle, 9 compresses and governs the shear deformation.

On the up cycles, 10 extends since the upper anchoring point is on the apex section of the joint that pushes away on the up cycles.

6. STATION 11 and 12 (SHEAR DEFORMATION)

The elastic behavior is highly dependent on cracking since the 2\1-yield cycles cause almost no deformation, but as cracks form on full yield cycles, the deformation takes a big jump.

The inelastic behavior is an extension of the response at full yield. On the down cycles, 11 extends and 12 compresses about equal amount.

On the up cycles, the extension of station 12 is dominant. This is due to apex section getting pushed outward and taking the upper anchorage point of station 12 with it.

7. STATIONS 13 and 14 (SHEAR DEFORMATION)

Before any cracking occurs, the shear strain is negative on both up and down cycles, similar to the behavior of stations 7 and 8. On the down cycles, the stations experience little compression, but on the up cycles, the experience a large negative shear, as can be confirmed by elastic analysis.

As expected, the shear deformation in the column is small, approximately an order of

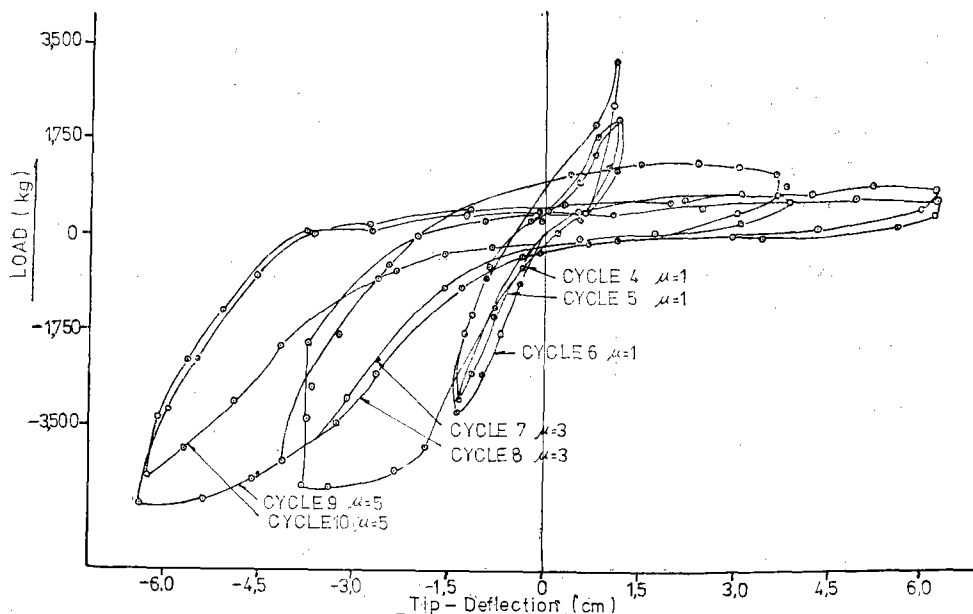


Fig. 5. Load Tip Deflection Curves

magnitude less than 9 and 10, and 11 and 12. But again as in station 12, station 14 extends on the up cycles due to the excursion of the excursion of the apex section on the up cycles.

8. STATION 15 (TIP DEFLECTION)

In the elastic region, it can be seen that recovery is almost 100%, indicating that almost all the energy being put into the system is being returned.

But on the early ductility 3 cycles, it can be seen that the system takes up more energy and recovery is no longer complete. The energy being lost to plastic deformation is evidenced by the width of the hysteresis loops.

As the ductility increases, the plastic deformation becomes complete, less energy is lost in the system and less force is required to obtain a certain deflection.

V. Conclusions

The major conclusions that can be drawn from the studies are as follows:

1. The joint exhibited a significant amount of stiffness up through cycle 6, i.e., The joint underwent simulated seismic loadings of $\mu=0.5$ and $\mu=1$ still displayed a fairly steep slope on the loaddeflection curve. Note that the predicted load at which flexural yielding occurred in the beam (part of the joint) corresponded closely to the load required to achieve a tip deflection. The beam portion of the joint had yielded by cycle and for each successive cycle (cycles 7, 8; $\mu=3$ and cycles 9, 10; $\mu=5$), the joint exhibited decreasing amounts of stiffness.

2. At $\mu=0.5$, a shear crack had developed in the joint region corresponding to a downward load. At $\mu=1.0$, shear cracks propagated and widened, note that tension cracks appeared after the $\mu=0.5$ cycles on all region of the joint, and that these tension cracks propagated and widened during the remaining cycles.

3. The moment curvature relation for joint region does not resemble a cyclic-loading-type pattern as would be expected, Note that the instantaneous slopes of the moment-curvature relations are much greater for the downward

loading portion of the cycles than for the upward loading portion. At $\mu=5.0$, the joint was expending large, non-uniform deformations for relatively small increments of load due to crack propagation and yield behavior of reinforcing steel.

4. In joint design, the weakest element of the RC structures is the beam. The beam showed much greater deflections than what had predicted at yield, therefore indicating that beam-column connections in the joint region are important areas to optimize design.

5. Instead of the re-entry point to apex cycle opening on the down half cycle, it opened on the up cycle. This can be explained by the fact that the crack initiated at the re-entry point rather than in shear at the center of the joint. Another probable cause for this maybe the small steel density near the re-entry point compared to the section at the top of the beam.

To pursue the study of joints further, the effects of radius of curvature on the re-entry point and the steel density in that region should be studied.

References

- 1) ACI Committee 318, Commentary on Building Code Requirements for RC, ACI 318-77, p. 55, Detroit, U.S.A., 1980
- 2) B. Bresler, Strength and Ductility Evaluation of Existing Low-rise RC Buildings-screending Method, EERC 76-1, p.78, UCB, 1976
- 3) D.L.N. Lee, Original and Repaired RC Beam-column Subassemblages Subjected to Earthquake-type Loading, Ph. D. Thesis, Univ. of Michigan, Michigan, U.S.A., 1976
- 4) E. Rosenblueth, Design of Earthquake Resistant Structures, p.46, John Wiley and sons, 1978
- 5) J. Fratt, Structural Repair of Earthquake Damaged Buildings, ASCE National Meeting, S.F., April, 1973
- 6) M. Murakami, Non-Linear Response Spectra for Probabilistic Seismic Design, EERC 75-38, UBC, Nov. 1975
- 7) P. Gulkan, The Inelastic Response of Repaired RC Beam-Column Connections, Sixth World Conference on Earthquake Eng., New Delhi, India, 1977
- 8) P.F. Rice and E.S. Hoffman, Structural Design Guide to the ACI Building Code, p.98, VNR CO., N.Y., 1980
- 9) S. Mahin and V. Bertero, Rate of Loading Effects on Uncracked and Repaired RC Members, EERC 72-9, UCB, Dec. 1972
- 10) V.V. Bertero, Design and Engineering Decisions, Failure Criteria, EERC 77-6, UCB, Feb. 1977
- 11) W.F. Chen, Theory of Beam-columns, p.247, M.G. Hill, 1979
- 12) S.B. Park, A study as the Response of R.C. Joint under simulated Seismic Conditions
- 13) T. Paulay, Ductility in Earthquake Resisting squat shearwalls, J. of ACI, Vol. 79, No. 4, 1982.